

The mechanics and behavior of Cliff Swallows during tandem flights

Ryan M. Shelton

A thesis submitted to the faculty at the University of North Carolina at Chapel Hill in partial fulfillment of the requirements for the degree of Masters of Science in the Department of Biology.

Chapel Hill
2014

Approved by:

Tyson L. Hedrick

Laura A. Miller

Kenneth J. Lohmann

© 2014
Ryan M. Shelton
ALL RIGHTS RESERVED

ABSTRACT

Ryan M. Shelton: The mechanics and behavior of Cliff Swallows during tandem flights
(Under the direction of Tyson L. Hedrick)

Cliff Swallows (*Petrochelidon pyrrhonota*) are highly maneuverable social birds that often forage and fly in large open spaces. Here I used multi-camera videography to measure the three dimensional kinematics of their natural flight maneuvers in the field. Specifically, I collected data on tandem flights, defined as two birds maneuvering together. These data allowed me to evaluate several hypotheses on their maneuvering flight performance. High speed turns were roll-based, but the magnitude of the centripetal force created in typical maneuvers varied only slightly with flight speed. In tandem flight the following bird copied the flight path and wingbeat frequency of the lead bird while maintaining position slightly above the leader. The lead bird tended to turn in a direction away from the lateral position of the following bird. Tandem flights vary widely in speed and duration and no single tracking strategy appeared to explain the course taken by the following bird.

ACKNOWLEDGEMENTS

I would like to thank Tyson Hedrick for mentoring me throughout my Masters, Laura Miller and Kenneth Lohmann for supporting me as committee members, Bill Kier for his willingness to help me with whatever I needed, George Lauder for helping me return to biomechanics, Joseph Thompson for introducing me to squid, Brandon Jackson for getting me up to speed on field flight recordings and his help with this thesis, Nick Deluga, Katherine Sholtis, and Amanda Lohmann for their assistance in collecting and analyzing the video data, and members of the Hedrick lab group for valuable discussion.

TABLE OF CONTENTS

LIST OF TABLES.....	vii
LIST OF FIGURES.....	viii
LIST OF SYMBOLS.....	ix
INTRODUCTION.....	1
MATERIALS AND METHODS.....	4
Swallow Recordings.....	4
Kinematic Analysis.....	6
Flight Model.....	10
Statistical Analysis.....	12
RESULTS.....	13
General Results.....	13
Turn Performance.....	15
Leader – Follower Comparisons.....	16
High Force Outlier.....	19
DISCUSSION.....	21
Flight Envelope.....	21
Turning Mechanics.....	23
Tandem Flights.....	25
Continuing Research.....	27

REFERENCES.....28

LIST OF TABLES

Table 1 – Flight Performance.....	8
-----------------------------------	---

LIST OF FIGURES

Figure 1 – Camera setup.....	5
Figure 2 - Structure-from-motion camera calibration.....	7
Figure 3 – Roll angle.....	9
Figure 4 - Modified coordinate axes for bird position.....	10
Figure 5 - Three-dimensional position and speed.....	14
Figure 6 - Turning mechanics.....	16
Figure 7 - Bird position.....	17
Figure 8 - Wingbeat phase offset	18
Figure 9 - Ratio of turn direction and speed	19
Figure 10 - Centripetal force outlier.....	20

LIST OF SYMBOLS

a	Acceleration	(m s ⁻²)
C_L	Coefficient of lift	(dimensionless)
F	Centripetal force	(body weights)
r	Radius of curvature	(m)
S	Wing area	(m ²)
θ	Roll angle	(degrees)
u	Flight speed	(m s ⁻¹)
v	Velocity	(m s ⁻¹)
w	Rate of change in heading	(degrees s ⁻¹)

INTRODUCTION

People have always been drawn to the impressive movements of graceful and powerful animals like dolphins and cheetahs. Over the last half century, the advancement of camera technology has allowed scientists to examine with ever-increasing detail the mechanics of how animals like these move. As frame rates and pixel counts have increased, scientists have spent more and more time looking at the diverse locomotion strategies employed throughout the animal kingdom (Biewener, 2003; Dickinson et al., 2000). This thesis will focus specifically on bird flight.

Behaviors in bird, bat, and flying insect species range in complexity from migratory cruising to high- and low-speed maneuvering during courtship, territory defense, and predator-prey interactions. Our understanding of the maneuverability of bats (Iriarte-Díaz and Swartz, 2008; Riskin et al, 2008) and insects (Card and Dickinson, 2008; Combes et al., 2012), along with birds (Tobalske, 2007), has grown rapidly over the last decade with each group developing new methods based on what has worked with other species. Most research to date on the mechanics of vertebrate flight have taken place in laboratories with wind tunnels (e.g. Tobalske and Dial, 1996; Ward et al., 2001; Spedding et al, 2003) or simple obstacle courses navigated at low speed (e.g. Swaddle, 1997; Warrick et al., 1998). The latter is a powerful approach for analyzing a specific maneuver because it allows for repeatable behaviors and optimally placed cameras to capture subtle details of the flight movements (e.g. Hedrick and Biewener, 2007; Iriarte-Díaz and Swartz, 2008; Ros et al., 2011). However, the behaviors elicited in laboratory environments may differ from those in natural environments, and are confined in speed and

scope by the size of the experimental space. To overcome these difficulties, and to better understand the dynamics of high-speed avian flight maneuvers, I used high speed video cameras to quantify flight maneuvers and conspecific interactions in natural environments.

I chose to study Cliff Swallows (*Petrochelidon pyrrhonota*) because they perform their well-known flight maneuvers in open spaces that permit easy recording with cameras. Cliff Swallows build nests in large colonies each spring in North America and migrate to South America for the winter (Brown and Brown, 1986). They are highly social passerines that perform many activities in groups including feeding, preening, gathering mud for nest-building, and perching (Emlen, 1952). As aerial insectivores, Cliff Swallows have evolved body and wing shapes consistent with changing direction (turning acceleration), and are therefore considered to be highly maneuverable (Brown and Brown, 1998).

Near nesting colonies, Cliff Swallows engage in one-on-one tandem flights, which appear to be aggressive chase sequences of high-speed maneuvers. These flights have been described as competitive interactions resulting from an intruder approaching a guarded nest (Brown and Brown, 1989). Because Cliff Swallows are conspecific nest parasites, such chases may serve to prevent the investment of energy in the rearing of adopted offspring (Petrie and Møller, 1991). These tandem flights have escalated to in-flight physical altercations including grappling with their feet, falling from flight while grappling, and disentangling just before reaching the water (personal observations, RMS). Therefore, I expect that the birds participating in tandem flights exhibit flight performance at the upper end of their performance envelope; these interactions appear to include the most elaborate maneuvers at relatively high speeds, compared to other flight behaviors near the nest colony (personal observations, RMS, TLH).

This study examines several specific questions related to these free-flight behaviors. What is the performance and maneuvering envelope of freely flying Cliff Swallows? What are the turning mechanics of Cliff Swallows in the field? What are the characteristics of these tandem flights? Why do these tandem flights occur? With respect to these questions I predict that I will see similar linear velocities and accelerations to those previously measured in laboratory-based obstacle courses and wind tunnels because performance envelopes in lab and the field should be the same (Warrick, 1998; Park et al., 2001); that roll angle is the primary variable determining the centripetal force and the rate of change in heading because this is the primary method of turning for both airplanes and dragonflies (Alexander, 1986); that these tandem flights are chases with a simple tracking or intercepting algorithm as exhibited by insects because we have seen birds physically fight in midair (Collett and Land, 1978; Olberg et al., 2000); and that these tandem flights are competitive interactions, with the lead bird taking action to avoid the following bird because the tandem flights tend to start near the nests in the season of nest guarding (Brown and Brown, 1989).

MATERIALS AND METHODS

Swallow Recordings

I recorded Cliff Swallow interactions of birds living in a colony of 30 to 60 under the NC highway 751 bridge over Jordan Lake, Chatham County, North Carolina, USA (35° 49' 42" N, 78° 57' 51" W). I placed 3 cameras on the shoreline underneath the bridge, each separated by approximately 3 meters, with the cameras aimed to monitor the same volume of space over the water next to their nest from slightly different angles (Fig. 1). I recorded on 26 separate mornings in the months of May and June of 2012 and May of 2013 collecting 100 Hz three-dimensional (3D) kinematic data for 32 tandem flights totaling 71 seconds. Each day I had a slightly different camera setup, varying due to the complex rocky shoreline, and recorded 1 to 3 good trials. Since I could not identify individual birds, I may have recorded some birds multiple times, but given the number of birds present and the time between trials it seems unlikely, so I chose to treat each tandem flight an independent event.

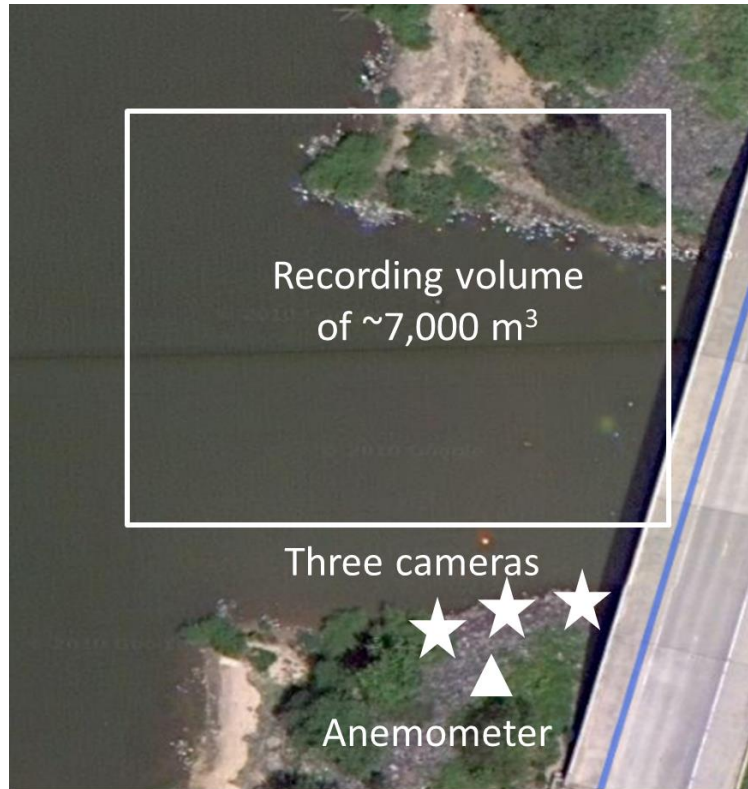


Figure 1. Camera setup. This is a satellite image (Google Maps, 2013) of the field site with stars showing the approximate location of the cameras, a white triangle marking the approximate location of the anemometer, and a white square showing the approximate recording volume.

To collect 3D field flight data in large outdoor volumes I worked with collaborators in the Hedrick lab and in Professor Margrit Betke's group at Boston University's Computer Science department to develop a structure-from-motion camera calibration routine which used a wand of known length to set the scale of the scene and provide an initial calibration; this was implemented as a custom MATLAB (The Mathworks, Natick, MA, USA) routine (Therialt et al., accepted). This preliminary calibration was then refined by adding individual swallows from calibration recordings as points of optical correspondence and applying a bundle adjustment optimization (Lourakis and Argyros, 2009) to the data and camera coefficients. The scene was then aligned to gravity by measuring the acceleration of a rock tossed through the scene, transforming the coefficients to place this acceleration vector on the z axis, and converted to a set

of direct linear transformation coefficients (DLT) for 3D analysis of bird trajectories (Hedrick, 2008). Camera recording positions varied slightly among trials, but typically set a recording volume of $\sim 7,000 \text{ m}^3$. Video data were collected using three synchronized high-speed cameras (N5r, Integrated Design Tools, Inc., Tallahassee, Florida, USA) recording 2336 x 1728 pixel images at 100 Hz. The calibrations had a median DLT residual of 1.23 pixels and a median 95% confidence interval in one dimension of 0.039 m.

I minimized the influence of wind by recording on days with little or no wind ($< 1.5 \text{ m s}^{-1}$). I measured the wind by placing a digital anemometer (HHF142, OMEGA Engineering, Inc, Stamford, Connecticut, USA) on the shoreline near the camera locations elevated between 2 and 6 meters above the water level. The birds were more exposed to wind than the anemometer flying over the exposed lake and at higher elevations. The anemometer was mounted on a gimbal allowing free rotation about the vertical axis; wind velocity was recorded at 1 Hz using a custom data logger which sampled the anemometer output, compass direction via a digital magnetometer and Global Positioning System location and time.

Kinematic Analysis

I manually digitized the head of each bird in each frame of each camera to determine the 3D bird positions with respect to time for each trial (Fig. 2) using the MATLAB package DLTdv5 (Hedrick 2008). Each trial includes two birds flying as a pair with one bird leading and the other bird following. I designate these birds as the lead bird and following bird, respectively, throughout the paper. These raw data were first processed by iteratively increasing the error tolerances of a quantic smoothing spline to affect a low pass filter at 1.0, 1.5, and 2.5 Hz to remove digitizing errors and within-wingbeat fluctuations in velocity and acceleration (Koenker et. al., 1994). The error variance was extracted from the 3D reconstruction uncertainty for each

data point. Varying the filter frequency did not impact any of our statistical conclusions and introduced only small variations in the data. Results in this paper are from the 1.5 Hz low pass filter unless otherwise noted. Derivatives of position with respect to time were calculated from the spline polynomial; I examined the first and second derivatives – velocity (\mathbf{v}) and acceleration (\mathbf{a}).

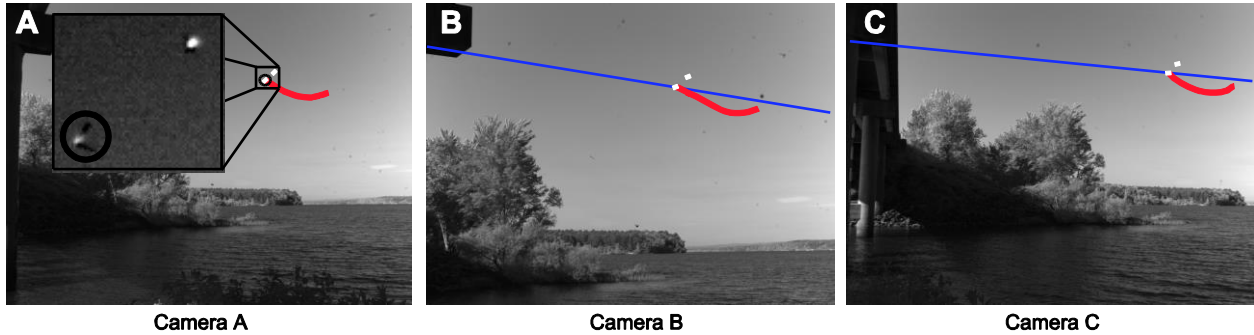


Figure 2. Structure-from-motion camera calibration. Example frames from the three synchronized cameras (A, B, C) placed along the shoreline to capture different views of the same volume of space. After completing our camera calibration procedure, I digitized the location of a bird in two or more camera views, shown here with the bird located in one camera (marked by the black circle in A) and the epipolar lines, (in blue in B and C) to find the exact 3D location of the bird at that time. The epipolar line defines the ray where the bird could be located in B and C given its location in A. The zoomed insert in A is contrast enhanced. White dots mark the location of the two digitized birds. The red lines show the flight path of the digitized bird over the preceding 1 second

I used the filtered position, \mathbf{v} , and \mathbf{a} data for all further calculations. I recorded the maximum instantaneous values from all of the data of speed, \mathbf{a} , magnitude of rate of change in heading, and magnitude of angular acceleration to document the maximum observed performance (Table 1). I calculated the mass specific power (not including drag) by

$$\frac{\text{power}}{\text{mass}} = \frac{\Delta(\text{kinetic} + \text{potential energy})}{\text{time} * \text{mass}}. \quad (1)$$

Mass on the right side of this equation will cancel allowing us to complete the calculation without knowing the mass of the bird. Since our swallows were not always maximizing power, I measured power over each possible 1 s interval for all of our trials and selected the largest mass

specific power from each trial. I then focused on the 10 trials with the largest power for further analysis.

Table 1. Flight Performance

Variable	Instantaneous maxima	Mean of trial means	Standard deviation of means
Speed (m s ⁻¹)	15.6	7.0	2.4
Acceleration (m s ⁻²)	78.1	13.6	6.6
Magnitude of rate of change in heading, w (deg s ⁻¹)	642	107	37
Magnitude of angular acceleration (deg s ⁻²)	7280	28	38
Tandem flight time (s)	4.71	2.28	1.14

I calculated the instantaneous radius of curvature (r) directly from \mathbf{v} and \mathbf{a} by

$$r = \frac{|\mathbf{v}|^3}{\sqrt{|\mathbf{v}|^2 |\mathbf{a}|^2 - (\mathbf{v} \mathbf{a}')^2}} \quad (2)$$

where \mathbf{a}' is the transpose of \mathbf{a} . I then calculated rate of change in heading (w) by

$$w = \frac{u}{r} \quad (3)$$

with u defined as flight speed. I extracted the frame and trial number of each local maxima in the graph of w with respect to time of the lead birds (number of peaks = 144) and tried to digitize the location of the extended wingtips in that frame (± 2 frames) to calculate roll angle (θ). I calculated θ as the angle between the line connecting the two wingtips and the line from one wingtip in the direction of the other wingtip but parallel to the horizontal plane (Fig. 3). I could only clearly identify the wingtip locations for 42 of the 144 turns. For these 42 turns I calculated centripetal force (F) in body weights by

$$F = \frac{u^2}{9.81r}. \quad (4)$$

I added a directional sign (positive = right, negative = left) for w , θ , and F .

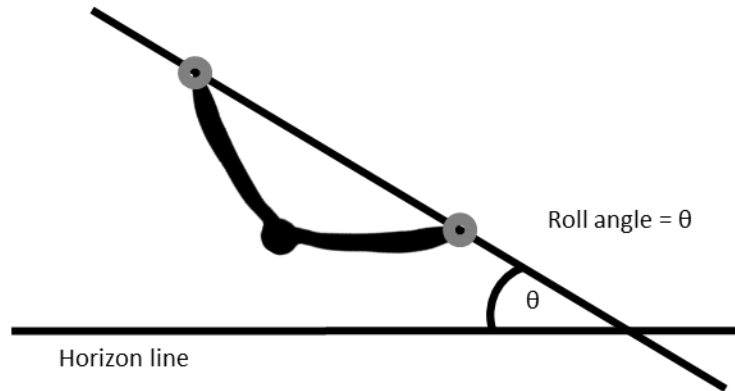


Figure 3: Roll angle. The roll angle was calculated as the angle between the line connecting the two wingtips and the line from one wingtip in the direction of the other wingtip but parallel to the horizontal plane. The wingtips, here marked with grey circles, were digitized at the frame of peak rate of change in heading.

To evaluate the relative body positions of the lead bird with respect to the following bird I defined a second coordinate system (x_b , y_b , z_b) where I rotated and shifted the original coordinate axes (x , y , z) to place the following bird at the origin flying up the y_b -axis for each video frame. This allowed us to use the lead bird's coordinates to define the forward distance as the y_b -coordinate, the vertical distance as the z_b -coordinate, and the lateral distance as the perpendicular distance from the y_b -axis to the lead bird position (Fig. 4).

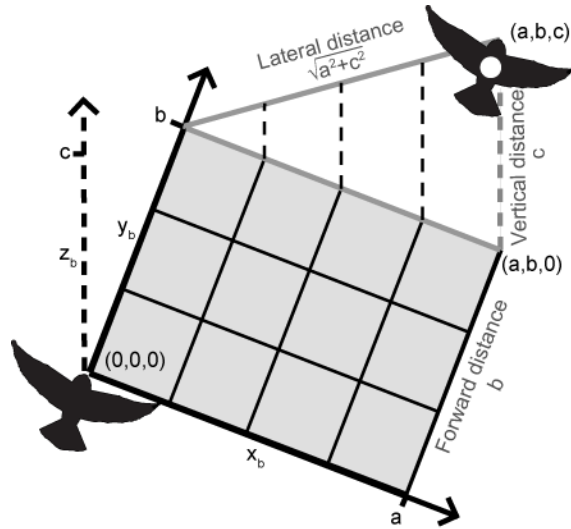


Figure 4: Modified coordinate axes for bird position. To measure the lateral, vertical, and forward distances between the lead and following birds I shifted and rotated the 3D axes of each frame so the following bird was at the origin flying along the y_b -axis. The vertical distance is the z_b -coordinate of the lead bird (c). The lateral distance is the perpendicular distance from the y_b -axis to the lead bird ($\sqrt{a^2 + c^2}$). The forward distance is y_b -coordinate of the lead bird (b).

I calculated the average wingbeat frequency by visually determining the frame number that each bird had its wingtips at their highest point for each wingbeat cycle. Of our 32 tandem flights, only 26 recordings clearly showed at least four consecutive wingbeats for both birds. To evaluate the relative timing of wingbeats of the lead bird and following bird I first evaluated each wingbeat separately. For each following bird wingbeat I calculated the number of frames until the next wingbeat started, set this wingbeat length equal to 360° , and noted the timing of the start of the lead bird's downstroke relative to the following bird's 360° wingbeat. For each trial I took the average timing of the lead bird's downstroke and treated the means from the 26 trials as independent data points.

Flight Model

To test if roll angle was the primary variable determining the centripetal force and the rate of change in heading I tested our measurements of F against simplified force models for

simple fixed-wing banked turns. I made progressively simplifying assumptions to isolate individual mechanisms. I started with the simple flight model of

$$\text{Lift} = \frac{1}{2} C_L S u^2 \quad (5)$$

with C_L = lift coefficient and S = wing area. I then calculated the lateral force F by finding the component of the lift vector redirected laterally by the roll angle (θ) by

$$F = \frac{1}{2} C_L S u^2 \sin(\theta). \quad (6)$$

If I drop $\frac{1}{2} C_L S$ from the equation by assuming that swallows use similar lift coefficient and wing area among all maneuvers, I am left with

$$F \propto u^2 \sin(\theta). \quad (7)$$

Since C_L drops out, it is unnecessary to determine what it is a function of. Alternatively, if Cliff Swallows modulate wing area and lift coefficient to match Lift (i.e. vertical force) to body weight and maneuver only by redirecting Lift, I expect:

$$F \propto \sin(\theta) \quad (8)$$

and thus lift proportional to θ after further linearization:

$$F \propto \theta. \quad (9)$$

As a third alternative, Cliff Swallows may turn by redirecting their Lift inward but also modulate coefficient of lift and wing area to maintain a vertical component equal to body weight. In this circumstance,

$$F \propto \tan(\theta) \quad (10)$$

which also linearizes to equation 9 for small θ . Thus, in our simplest model I would expect to see a correlation for F with respect to θ . I would also expect this correlation to increase when I substitute some combination of u , u^2 , and $\sin(\theta)$ or $\tan(\theta)$ for θ , moving toward the more

complete models. In addition, I would expect an improved correlation from substituting the horizontal component of centripetal force (by $F \cos(\theta)$) for F .

Statistical Analysis

I used several different statistical methods to evaluate our data. To measure the correlations between each paired combination of F , θ , and w I calculated a linear regression, a correlation coefficient (r^2), and a p-value. I used a t-test to evaluate the null hypotheses that the lead bird turns toward and away from the following bird in equal portions of time. A t-test was also used to evaluate the null hypothesis that the lead bird and following bird have equal mean velocities. I used MATLAB for these statistics treating each tandem flight as a single independent trial.

To evaluate the relative vertical distance, defined by Z_b in Figure 2, I used a generalized estimating equation to test the null hypothesis that the vertical distance is equal to 0 using R with the geepack library (R Foundation for Statistical Computing, Vienna, Australia; Zeger et al., 1988). I evaluated the relative wingbeat timing for the lead bird and following bird using a Rayleigh Test using Oriana (Kovach Computing Services, Wales, UK; Brazier, 1994).

RESULTS

General Results

In each recorded tandem flight the following bird copied the movements of the lead bird in 3D space and in the x, y, and z position components independently (e.g. Fig. 5). Copying behavior appeared to be independent of variation in distance travelled, interaction time, elevation change, and turning rate among tandem flights. I recorded the mean and maximum speed, acceleration, rate of change in heading (here the direction of the 3D velocity vector), angular acceleration (here the derivative of the magnitude of the rate of change in heading), and flight time of our trials (Table 1). The mean of the trial mean speeds (7.0 m s^{-1}) is less than half the maximum observed speed (15.6 m s^{-1}) showing that these interactions often occur below peak linear speed performance. Flight speeds often drop below the optimal cost of transport flight speeds, as given by the speed of minimum flapping frequency for Barn Swallows in a wind tunnel. The mean power of the 10 trials with the highest mass specific power ($\pm\text{SD}$) was $21.2 \pm 4.5 \text{ W kg}^{-1}$ (see Eqn 1). These tandem flights were short, lasting 2.28 s on average.

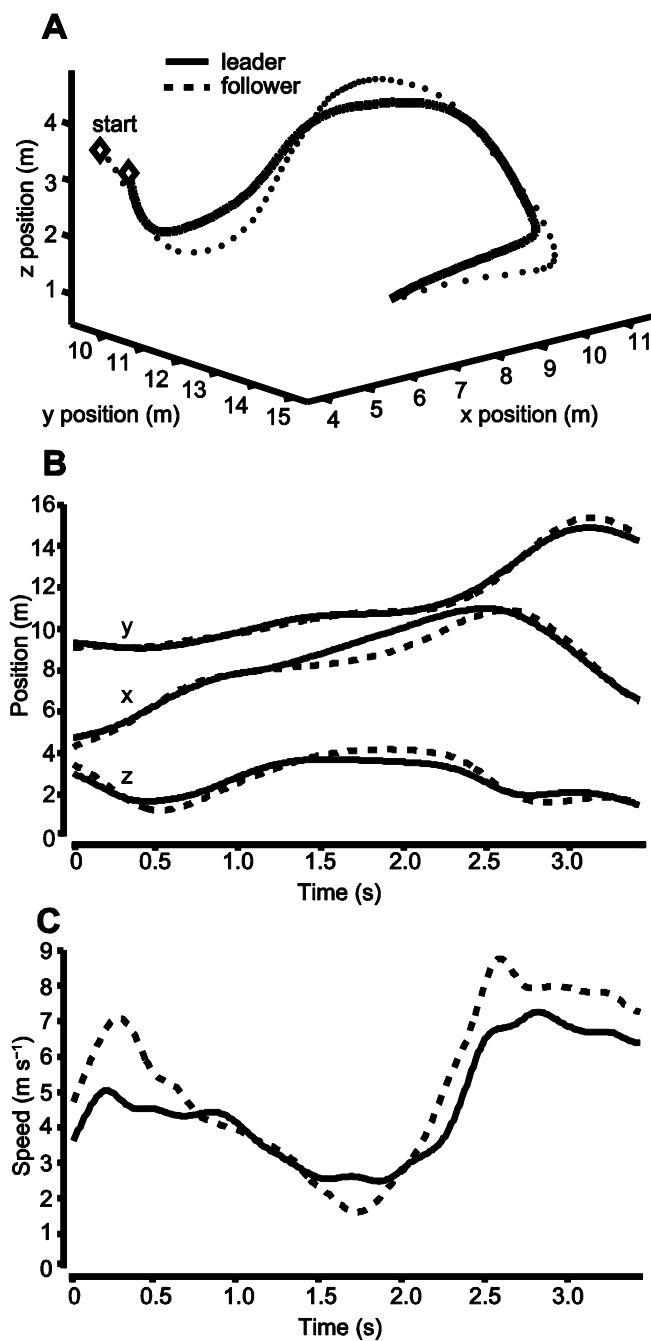


Figure 5: Three-dimensional position and speed. (A) The 3-dimensional positions of a lead and following bird for a tandem flight starting at the diamonds in the upper left. The z-axis is aligned with gravity. (B) The x, y, and z components of the position with respect to time. The following bird copies the lead bird's position closely in each component. (C) The speed of the following bird is slightly faster than the lead bird and the speed in this tandem flight ranges from 1.6 to 8.8 m s⁻¹.

Turn Performance

I measured or calculated the roll angle (θ), flight speed (u), rate of change in heading (w), and centripetal force (F) of 42 lead bird turns, and I found strong and significant correlations between θ and w ($r^2 = 0.69$, $p < 0.001$, Fig. 6A), θ and F ($r^2 = 0.64$, $p < 0.001$, Fig. 6B), and F and w ($r^2 = 0.82$, $p < 0.001$, Fig. 6C). I did not find a significant correlation between u and F ($r^2 = 0.064$, $p = 0.168$, Fig. 5D). Several birds exhibited extreme performance. One turn has a θ of 116° because the bird flew inverted for 0.05 s. There was also one turn with an apparent F outlier producing 7.8 body weights of force, more than twice the force of any other observed turn – see further examination of this result below. Roll angle (θ) was the single variable that explained the greatest variation in F compared to any combination of u , u^2 , $\sin(\theta)$, and $\tan(\theta)$ as suggested by the simple flight model presented in the methods. Exchanging the horizontal component of centripetal force (computed as $F \cos(\theta)$) for F also decreased the correlation.

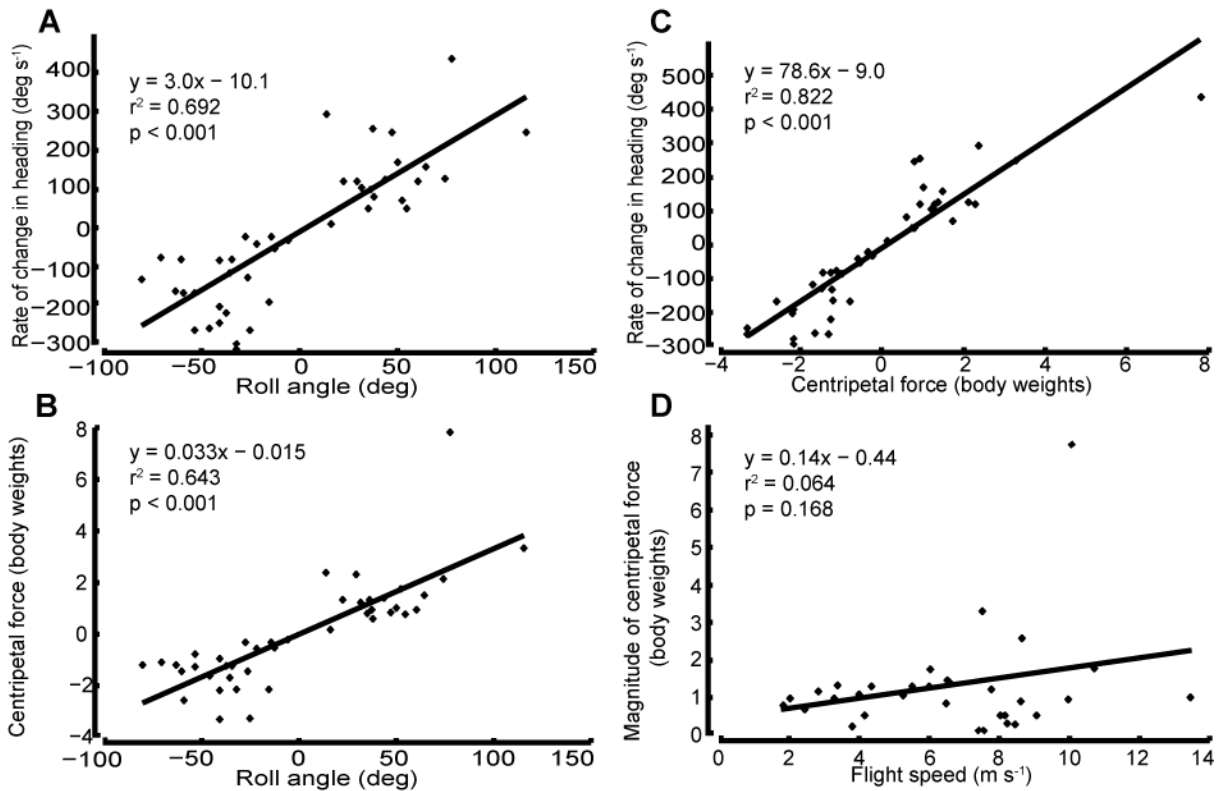


Figure 6: Turning mechanics. For 42 turns I compared (A) rate of change in heading with respect to roll angle, (B) centripetal force with respect to roll angle, (C) rate of change in heading with respect to centripetal force, and (D) flight speed with respect to centripetal force. For roll angle, rate of change in heading, and centripetal force, positive = right and negative = left. A, B, and C have high correlations and significant p-values but D has a near zero correlation and is insignificant. Two points of interest include the inverted turn with a roll angle of 116° and the centripetal force of 7.8 body weights. Excluding the force outlier from the calculation for D provides the same conclusion ($y = 0.024x + 0.921$, $r^2 = 0.010$, and $p = 0.605$).

Leader – Follower Comparisons

I observed a variety of following positions with respect to the lead bird, but there was a tendency to avoid following directly behind the leader (Fig. 7A), and a statistically significant trend of aiming above the leader (Fig. 7B, using a generalized estimating equation, $p = 0.03$).

The mean wingbeat frequencies of the lead bird (12.3 ± 1.7 Hz) and following bird (12.4 ± 1.6 Hz) were statistically indistinguishable. The following bird, on average, started its downstroke less than $\frac{1}{4}$ wingbeat after the lead bird (Fig. 8). The outer circle represents the full wingbeat cycle of the following bird and each point is the mean timing of the start of the downstroke of the

lead bird. Perfect synchronization would be represented by all points positioned at 0° . The non-random distribution (Rayleigh Test; $r = 0.38$, $p = 0.021$, $n = 26$) averaged 332° (95% CI: 292° to 11°).

On average, the lead bird turned away from the following bird 65% of the tandem flight (Fig. 9A, t-test, $p < 0.001$). The following bird had a longer flight path and flew 6% faster on average than the lead bird (t-test, $p = < 0.001$, Fig. 9B).

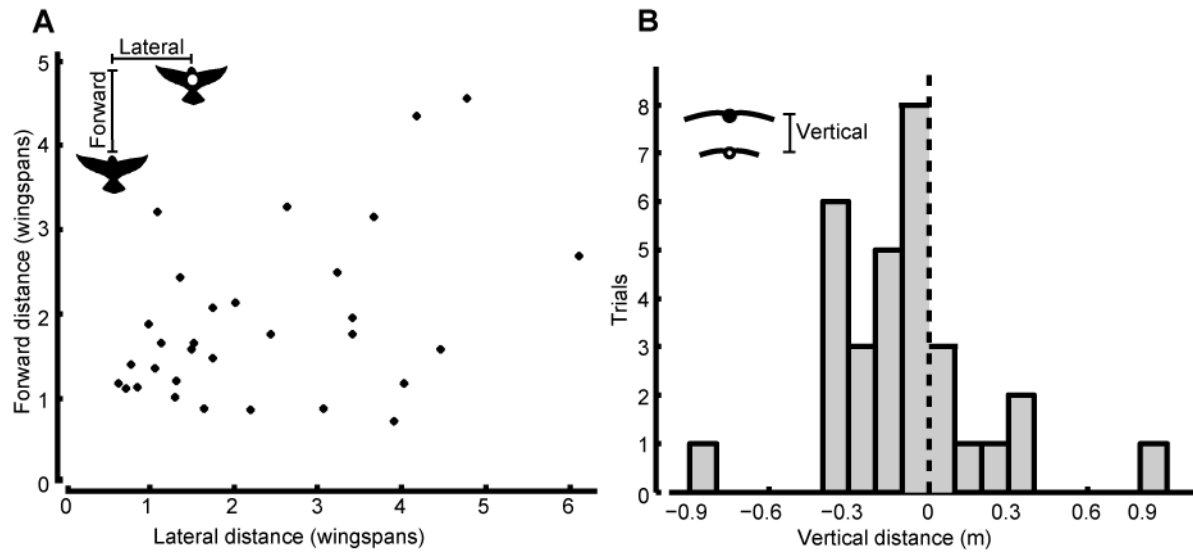


Figure 7: Bird position. (A) Each marker represents the mean location of the lead bird with respect to the following bird through one entire tandem flight sequence ($n=32$). (B) The histogram shows the mean vertical location of the leader for each trial with negative distances defined by the leader being below the follower's trajectory. The dashed line at zero shows the expected mean if the follower was aiming in line with the leader. This distance is significantly less than zero using a generalized estimating equation (GEE) with $p=0.03$ meaning the follower tends to aim above the leader.

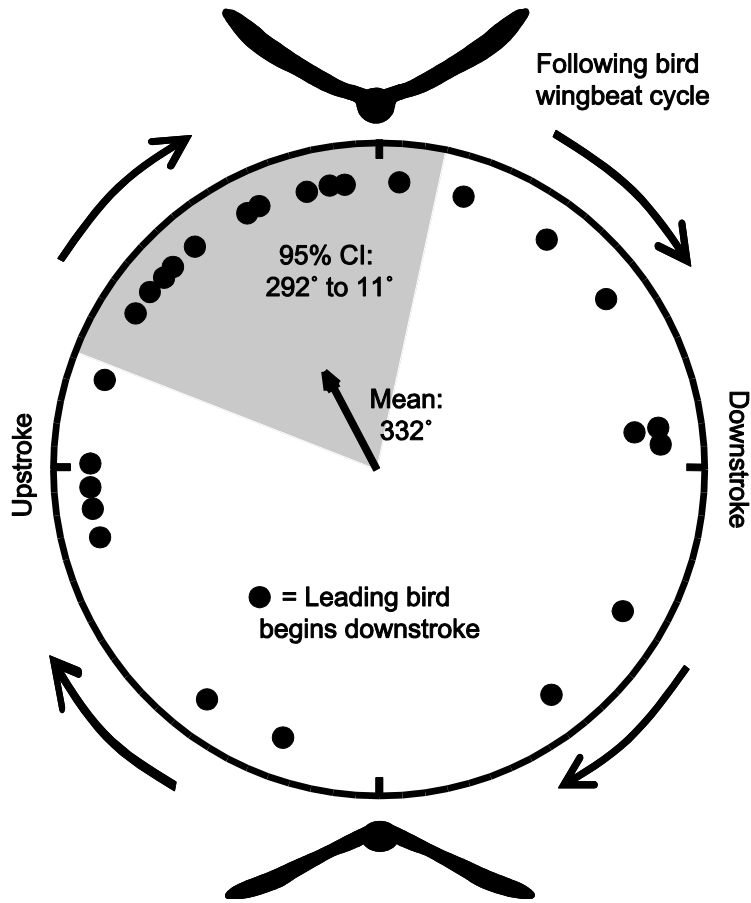


Figure 8: Wingbeat phase offset. Here I show the phase offset of the beginning of downstroke among the follower and leader. The outer circle represents the full wingbeat cycle of the following bird. For each wingbeat cycle I observed the timing in frames of the start of the lead bird's downstroke relative to the following bird's wingbeat cycle. Each dot is the mean timing of the start of the lead bird's downstroke for a single trial. If the top of this graph is defined as zero degrees and numbers increase clockwise, the mean of the trial means is 332 degrees ($r = 0.38$, $p = 0.021$, $n = 26$) with the shaded region showing the 95% confidence interval. This is a significant result supporting a non-random distribution of wingbeat phasing between the two birds with the lead bird tending to flap just before the following bird.

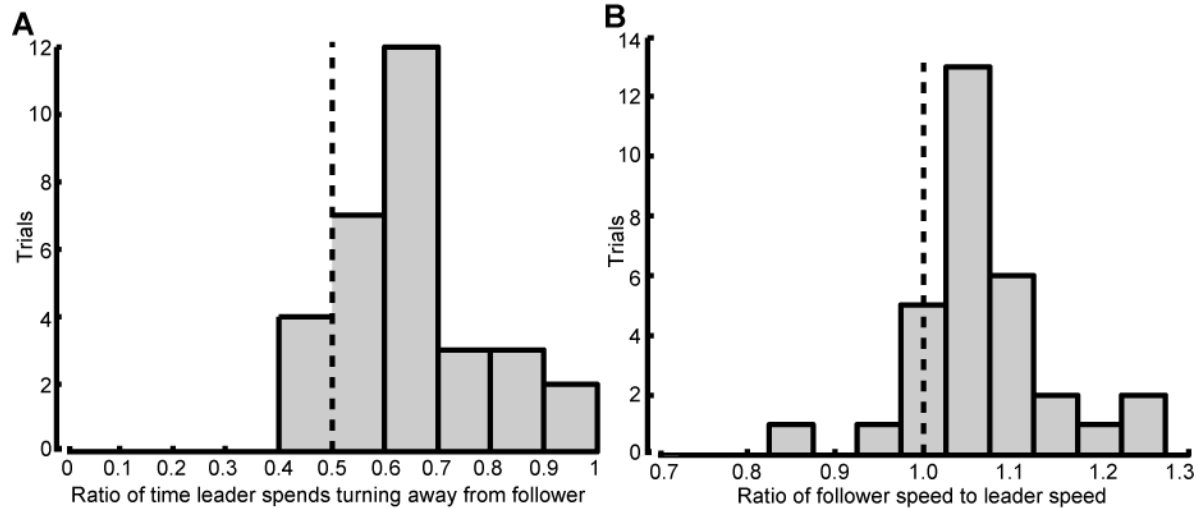


Figure 9: Ratio of turn direction and speed (A) For each trial I measured the ratio of time that the lead bird is turning away from the following bird and found the leader turning away for the majority of time in 27 of 31 trials. The dashed line at 0.5 shows the expected mean if the turn direction was random. The data mean is significantly different from 0.5 by a t-test (mean = 0.65, SE = 0.03, $p < 0.001$). (B) The ratio of the mean followers speed to mean leaders speed shows that the lead bird is flying faster than the following bird in only 2 of 31 trials suggesting that the following bird is flying faster to adjust to an unpredictable flight path. The dashed line at 1.0 shows the expected mean if both birds had the same mean velocity. These data are significantly different from 1.0 by a t-test (mean = 1.06, SE = 0.01, $p < 0.001$).

High Force Outlier

I estimated a centripetal force of 7.8 body weights in one turn, more than double any other turn I quantified (Fig. 10). This sequence included a number of factors that may have contributed to the high force measurement: a large θ of 78° , a fast speed of 14.6 m s^{-1} immediately preceding the turn, a quick reduction in speed by 4.5 m s^{-1} during the time of the turn, and the possibility of ground effect enhancing aerodynamic forces since the entire tandem flight occurred just above the water surface.

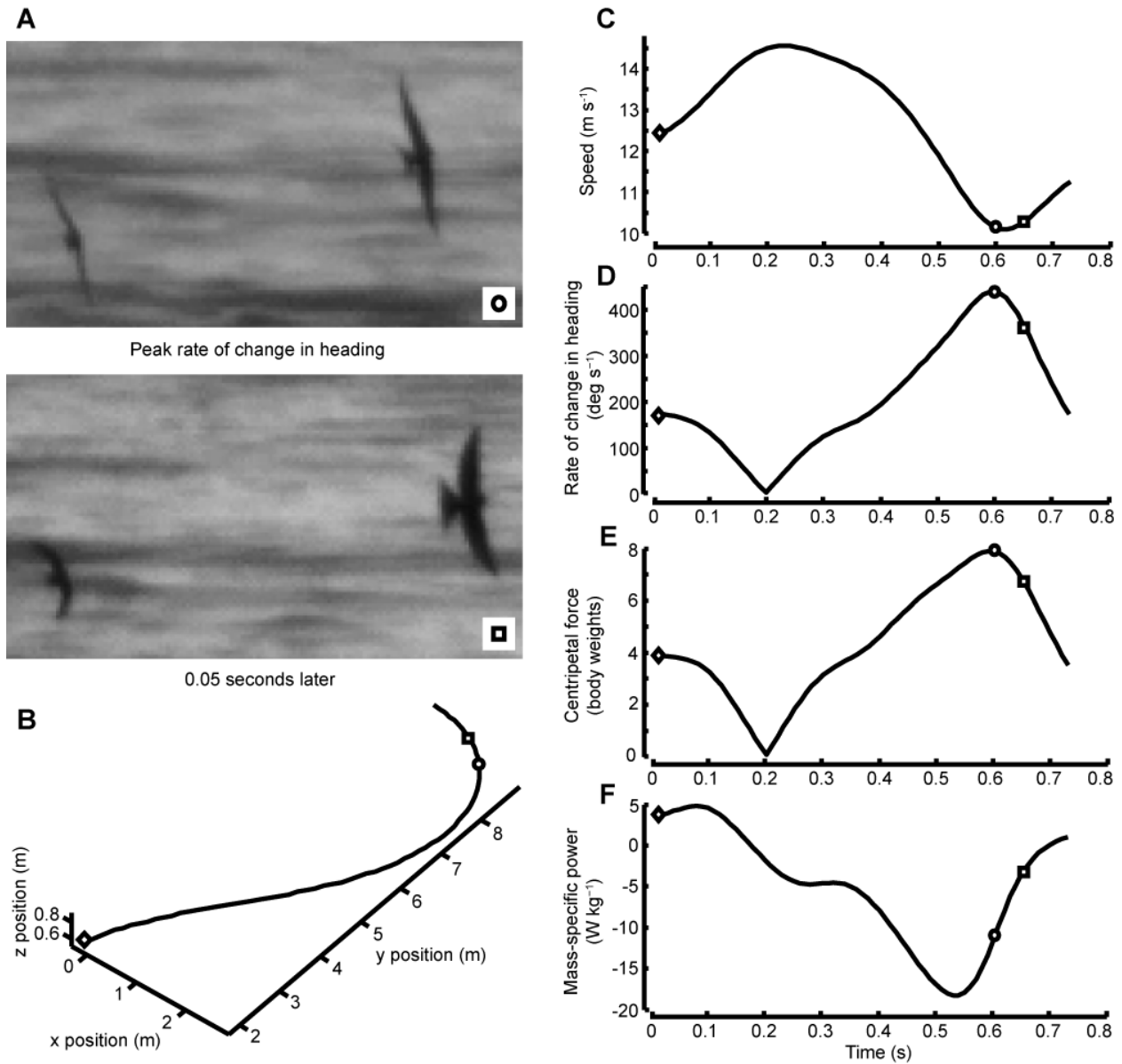


Figure 10: Centripetal force outlier. This lead bird turn had a centripetal force twice as large as any other observed turn, and rate of change in heading 35% larger than any other turn. (A) These images show the moment of peak rate of change in heading, and the moment 0.05 seconds later. The circle and square markers in the lower right corners are presented in the graphs to show the timing of these images. The contrast in these images has been enhanced. The 3D position (B), velocity with respect to time (C), rate of change in heading (D), centripetal force (E), and mass-specific power (F) are presented with each sequence starting at the diamond.

DISCUSSION

Flight Envelope

Compared to the single turn produced by 7.8 times body weight force, most trials included performance well within the known flight envelope for Cliff Swallows and related species. While Cliff Swallow flight has not been examined in a wind tunnel to the best of our knowledge, I can compare our data to previous research on Barn Swallows (*Hirundo rustica*). Flight speeds of two Barn Swallows ranged from 3.4 to 14.0 m s⁻¹ in a wind tunnel (Park et al, 2001). I found that the time averaged flight speeds of Cliff Swallows had a similar range and identical maximums (2.8 to 14.0 m s⁻¹) despite differences in wing shape and body size between the two species. Since I measured open-area flights, and birds were free to fly at self-chosen speeds, I can also look at the maximum instantaneous flight speeds over 0.01 second intervals. Cliff Swallows flew at instantaneous speeds up to 15.6 m s⁻¹. It was surprising that these tandem flights occurred at such a large range of speeds. Given the expectation that these were competitive chases, I would expect most of these flights to maximize their velocity threshold, but that is not what we observed. I will discuss the possible implications of this further in the Tandem Flights section that follows.

Cliff Swallows have been examined during linear escape flights. Warrick found the linear acceleration in four different swallow species ranged from 5.45 to 8.92 m s⁻², with Cliff Swallows averaging 5.98 m s⁻², when measuring swallows starting from rest and flying in a straight horizontal line (Warrick, 1998). Cliff Swallows in tandem flights had an average linear acceleration of 13.6 m s⁻², but unlike the horizontal flight test experiment, some of the swallows

in our study were able to descend, using potential energy as well as muscle work to accelerate, and potentially took advantage of other environmental factors like pressure gradients and vortices. Calculating the mass-specific power output (not including drag, see Eqn 1 in methods) can account for added acceleration due to gravity and provides a more relevant comparison between the different behaviors. Warrick's Cliff Swallows started from rest and accelerated to 7.26 m s^{-1} in 4 m, resulting in a mass specific power of 22.8 W kg^{-1} . Swallows in tandem flights, starting from a wide range of speeds, averaged 21.2 ± 4.5 (mean \pm SD) W kg^{-1} . This power estimate would increase if I included drag and a full aerodynamic model. Thus, the freely flying swallows exhibited approximately the same mass specific power as was found in the capture and release study of escape accelerations, even though the conditions of these measurements were drastically different. The level acceleration experiment with recently captured wild swallows was designed to elicit maximum performance; the similar results from freely behaving birds suggests that Cliff Swallows may use most, if not all, of their performance envelope on a day to day basis.

The vertical takeoff power outputs of Blue-Breasted Quail (47.0 W kg^{-1} ; Askew et al, 2001) and Gray Jay (27.7 W kg^{-1} ; Jackson and Dial, 2011) are larger (43.6 g , 68.9 g , respectively) than our measured Cliff Swallow free-flight power. Aerodynamic and allometric theory would predict that smaller Cliff Swallows should have higher power outputs than the other, larger, species (Pennycuick 1975), which may suggest that our Cliff Swallow values are not maximal. Alternately, since swallows are not acceleration specialists and can often use potential energy to enhance flight maneuvers and prey capture attempts, Cliff Swallows may simply have a lower maximal capability for muscle powered acceleration.

Based on the rate of change in heading and the magnitude of the angular acceleration in tandem flight turns, I estimated the aerodynamic centripetal forces developed by Cliff Swallows

(Table 1, Fig. 4). Similar field measurements during high-speed flight have only been reported for the courtship dives of Anna's hummingbirds, which experienced a gravity assisted centripetal force of 9 body weights on average (Clark, 2009). This is only slightly higher than the 7.8 body weights maximum reported here, but much greater than our median magnitude of centripetal force of 1.0 body weights. It is likely that the number of documented turning kinematics in the literature will rapidly increase over the next 10 years, providing more of a scaling context for these results. However, I was somewhat surprised to find similar maximum flight forces in the natural flight maneuvers of swallows and hummingbirds since the swallows are approximately three-fold larger in mass than the hummingbirds and also differ greatly in ecological niche and typical flight behavior.

I also compared these centripetal forces to experiments on pigeons and cockatoos completing 90° turns through L-shaped corridors at low speeds in laboratory maneuvering tests. Pigeons flying at 3.3 m s⁻¹ with a turning radius of ~1.0 m produced a maneuver-averaged centripetal force of 10.9 body weights (Ros et al., 2011); Rose-Breasted Cockatoos making similar turns at 3.01 m s⁻¹ with a radius of 0.92 m produced 9.8 body weights (Hedrick and Biewener, 2007). These larger birds are producing larger forces than our Cliff Swallows which produced less than 2.0 body weights at similar speeds and likely reflect the severe spatial constraints the birds were forced to maneuver under in the laboratory studies.

Turning Mechanics

As I predicted, roll angle (θ) strongly correlated with both F and w . Swallows produced about 3.0 body weights of centripetal force at a 90° roll angle (Fig. 6B), independent of flight speed (Fig. 6D). An ideal fixed-wing glider that could transfer all aerodynamic force (lift) into centripetal force would be able to produce 1.0 body weights of centripetal force at a 90° roll

angle, assuming no change in coefficient of lift. These differences are reasonable given the swallows' expected ability to vary coefficient of lift and their continued wing flapping through most of the turns. I was unable to determine many details of wing flapping kinematics such as wing extension, stroke amplitude and gait changes.

The basic mechanics of the Cliff Swallow turns were different from those expected for a fixed-wing glider. In the methods I derived a simple linearized expression for a simple fixed-wing banked turn to $F \propto \theta$ (Eqn 9 in methods). Stepping back two equations in our model to $F \propto u^2 \sin(\theta)$ (Eqn 7 in methods), I expected to see our correlations increase. Instead, when I substituted any combination of u , u^2 , $\sin(\theta)$ or $\tan(\theta)$ for θ , our correlations decreased in strength. When I tried substituting the horizontal component of centripetal force ($F \cos(\theta)$) for F I also saw a decrease in correlations. Essentially, the lateral force produced by swallows is proportional to roll angle, indicating a banked turn, but nearly independent of forward velocity. This indicates that swallows rarely use large lift coefficients when turning while flying fast, despite their apparent ability to do so as demonstrated by the 7.8 g turn discussed earlier. In that maneuver the bird also slowed rapidly, presumably due to the induced drag associated with the large lift coefficient, demonstrating the costs of high force turns. Furthermore, flapping provides another avenue for producing larger forces than expected from forward speed alone and could also account for the absence of a forward speed relationship, especially at slow speeds. The majority of turns recorded here were flapping maneuvers. The absence of improvement when using $\sin(\theta)$ or $\tan(\theta)$ to examine a specific lift-based turn model, either one where the bird produces no additional force or produces additional force adequate to maintain perfect weight support suggests that swallows may compromise between the two, producing some additional force but not enough for weight support at larger θ .

Finally, our large filming volume precluded us from being able to discern detailed wingbeat kinematics; higher resolution or closer image captures of swallows turning in high speed free flight will be necessary to detail the exact motions of the swallow wings and body that produce F . The maneuvers examined with this model are a subset of the possible flight maneuvers and turning mechanisms available to swallows. For example, vertical maneuvers were uncommon during tandem flights, and therefore the maneuvering model comparisons are necessarily only tested against approximately level turns in the ~ 3 to ~ 16 m s^{-1} speed range.

Tandem Flights

Our initial hypothesis that all of these tandem flights were chases including a simple tracking or intercepting strategy was not supported. Instead of aiming at the lead bird or in front of the lead, the follower tends to fly parallel to the lead bird while offset to one side or the other, with the result that the following bird generally copies the flight path of the lead bird. These data do not support the assumption that the following bird had the ‘goal’ of making contact with the lead bird. However, the tendency of the lead bird to turn away from the follower and for the follower to fly faster than the leader (Fig. 9) does support the hypothesis that these flights are competitive interactions. Cliff Swallows are highly cooperative populations but they also have high intraspecific brood parasitism (Brown and Brown, 1989), which could invoke competitive interactions. The flights I recorded mostly occurred in May and early June, coinciding with nest building and egg laying. Additionally, while I could not determine the location of the birds relative to the home nest, most of the flights began very close to nests (personal observation RMS), further suggesting that these tandem flights were acts of nest defense from conspecifics. The large variation in speed, length, bird position, and turning behaviors among trials may represent varying degrees of relative competitiveness of the two birds involved, with some birds

being driven away more easily and other birds requiring more aggressive pursuit. The offset position of the follower may provide an aerodynamic advantage of reducing flight cost (Portugal et al., 2014), or a behavioral advantage of allowing the follower to be seen or to cut off turns towards the nest. These tandem flights might be part of an escalation process progressing towards physical combat. If so, the birds would attempt to send signals to resolve the conflict with minimal energy loss which would explain why most turns are well below the maximum observed turning force since the maximum force turn observed here imposed a substantial energy cost.

Wingbeat frequency and the timing of wingbeat cycles were unexpectedly synchronized, with a slight phase shift, in lead and following birds. Since the following bird is copying the lead bird's maneuvers and flight path, it makes sense that the follower would delay its wingbeat in order to first observe the leader's maneuver. On average, our data show the lead bird starting its downstroke 332° into the follower's wingbeat cycle (Fig. 8). In other words, the follower's wingbeat starts 28° , or approximately 6 ms, after the leader's wingbeat cycle. This response time is fast in comparison to dragonflies (29 ms; Olberg et al., 2007), hoverflies (~20 ms; Collett and Land, 1978), houseflies (~30 ms; Land and Collett, 1974), dolichopodid flies (~15 ms; Land, 1993), and bats (120 ms; Ghose et al., 2006). Thus, it is unlikely that the following birds were simply responding to the timing of the lead birds' downstroke with each wingbeat cycle. Alternatively, the follower may be reacting to whole-body movements of the lead bird, and may require slightly more than the duration of a wingbeat cycle (81 ms total for wingbeat plus 6 ms delay) to receive, interpret, and react to the input. In other words, the follower's latency of reaction may mean that what appears as a phase shift of $\sim 30^\circ$ may actually be a phase shift of $\sim 390^\circ$. If the follower exhibited a consistent tracking strategy I would be able to distinguish

between the two phase offset possibilities by extracting the response latency between the leader and follower. However, since the swallows appear to use different tracking strategies depending on context, I cannot use this information to conclusively separate the two possibilities, although a 390° offset is more consistent with typical sensory response times as noted above.

Continuing Research

In this paper I was able to find some clear conclusions about the flight envelope and turning mechanics of Cliff Swallows flying in the field, but there is still a lot to learn about the behavioral component of these tandem flights. While many aspects of these flights appear to be competitive, the evidence is not conclusive. If I could explain the benefit of these tandem flights for each bird we could probably also explain each bird's strategy, and then further evaluate how effective each bird is at accomplishing its goal. One way to get this data would be to catch several of these birds, attach easy to see anklets, take physical measurements of each bird, identify their sex, release them, and then track their behavioral patterns over a series of days or weeks. This new study could clarify if certain birds are more likely to lead or follow, if each bird performs the behavior with the same frequency, if sex is an important characteristic in these chases, if the same two birds pair off most of the time or if the pairings are more randomly distributed, and if there is a particular physical characteristic that predicts success or failure. Once a more comprehensive behavioral study of tandem flights was complete, other biomechanical information like response latencies and following algorithms should be easier to decipher.

REFERENCES

- Alexander, D. E. (1986). Wind tunnel studies of turns by flying dragonflies. *J. Exp. Biol.* 122, 81-98.
- Askew, G. N., Marsh, R. L., & Ellington, C. P. (2001). The mechanical power output of the flight muscles of blue-breasted quail (*Coturnix chinensis*) during take-off. *J. Exp. Biol.* 204, 3601-3619.
- Biewener, A. A. (2003). *Animal locomotion*. Oxford University Press.
- Brazier, K. T. S. (1994). Confidence intervals from the Rayleigh test. *Mon. Not. R. Astron. Soc.* 268, 709.
- Brown, C. R., & Brown, M. B. (1986). Ectoparasitism as a cost of coloniality in cliff swallows (*Hirundo pyrrhonota*). *Ecology*. 67, 1206-1218.
- Brown, C. R., & Brown, M. B. (1989). Behavioural dynamics of intraspecific brood parasitism in colonial cliff swallows. *Anim. Behav.* 37, 777-796.
- Brown, C. R., & Brown, M. B. (1998). Intense natural selection on body size and wing and tail asymmetry in cliff swallows during severe weather. *Evolution* 52, 1461-1475.
- Card, G. and Dickinson, M. (2008). Performance trade-offs in the flight initiation of *Drosophila*. *J. Exp. Biol.* 211, 341-353.
- Clark, C. J. (2009). Courtship dives of Anna's hummingbird offer insights into flight performance limits. *Proc. R.Soc.B.* 276, 3047-3052.
- Collett, T. S., & Land, M. F. (1978). How hoverflies compute interception courses. *J. Comp. Physiol.* 125, 191-204.
- Combes, S.A., Rundle, D.E., Iwaski, J.M. and Crall, J.D. (2012). Linking biomechanics and ecology through predator-prey interactions: Flight performance of dragonflies and their prey. *J. Comp. Physiol.* 215, 903-913.
- Dickinson, M. H., Farley, C. T., Full, R. J., Koehl, M. A. R., Kram, R., and Lehman, S. (2000). How animals move: an integrative view. *Science* 288, 100-106.
- Emlen, J. T. (1952). Social behavior in nesting cliff swallows. *Condor* 54, 177-199.
- Google Maps (2013). [Highway 751 at Jordan Lake, Chattam, NC] [Satellite map] Retrieved from <https://www.google.com/maps/place/Jordan+Lake/@35.8283539,-78.9643201,128m/data=!3m1!1e3!4m2!3m1!1s0x89acbff6ec7806fd:0x7fc03219c9a7d8d>

- Ghose, K., Horiuchi, T. K., Krishnaprasad, P. S., & Moss, C. F. (2006). Echolocating bats use a nearly time-optimal strategy to intercept prey. *PLoS Biol.* 4, e108.
- Hedrick, T. L. (2008). Software techniques for two-and three-dimensional kinematic measurements of biological and biomimetic systems. *Bioinspir. Biomim.* 3, 034001.
- Hedrick, T. L., & Biewener, A. A. (2007). Low speed maneuvering flight of the rose-breasted cockatoo (*Eolophus roseicapillus*). I. Kinematic and neuromuscular control of turning. *J. Exp. Biol.* 210, 1897-1911.
- Iriarte-Díaz, J., Swartz, S. M. (2008). Kinematics of slow turn maneuvering in the fruit bat *Cynopterus brachyotis*. *J. Exp. Biol.* 211, 3478-3489.
- Jackson, B. E., & Dial, K. P. (2011). Scaling of mechanical power output during burst escape flight in the Corvidae. *J. Exp. Biol.* 214, 452-461.
- Koenker, R., Ng, P., & Portnoy, S. (1994). Quantile smoothing splines. *Biometrika*, 81, 673-680.
- Land, M. F. (1993). Chasing and pursuit in the dolichopodid fly *Poecilobothrus nobilitatus*. *J. Comp. Physiol. A* 173, 605-613.
- Land, M. F., & Collett, T. S. (1974). Chasing behaviour of houseflies (*Fannia canicularis*). *J. Comp. Physiol.* 89, 331-357.
- Lourakis, M. I., & Argyros, A. A. (2009). SBA: A software package for generic sparse bundle adjustment. *ACM Trans. on Math. Software.* 36, 1-30.
- Olberg, R. M., Worthington, A. H., & Venator, K. R. (2000). Prey pursuit and interception in dragonflies. *J. Comp. Physiol. A*, 186, 155-162.
- Olberg, R. M., Seaman, R. C., Coats, M. I., & Henry, A. F. (2007). Eye movements and target fixation during dragonfly prey-interception flights. *J. Comp. Physiol. A*. 193, 685-693.
- Park, K. J., Rosén, M., & Hedenström, A. (2001). Flight kinematics of the barn swallow (*Hirundo rustica*) over a wide range of speeds in a wind tunnel. *J. Exp. Biol.* 204, 2741-2750.
- Pennycuik, C. J. (1975). Mechanics of flight. In *Avian Biology*, vol. 5 (ed. D. S. Farner and J. R. King), pp. 1-75. New York: Academic Press.
- Petrie, M., & Møller, A. P. (1991). Laying eggs in others' nests: intraspecific brood parasitism in birds. *Trends Ecol.Evol.* 6, 315-320.

- Portugal, S. J., Hubel, T. Y., Fritz, J., Heese, S., Trobe, D., Voelkl, B., Hailes, S., Wilson, A. M., Usherwood, J. R. (2014). Upwash exploitation and downwash avoidance by flap phasing in ibis formation flight. *Nature*, 505, 399-402.
- Riskin, D. K., Willis, D. J., Iriarte-Díaz, J., Hedrick, T. L., Kostandov, M., Chen, J., Laidlaw, D. H., Breuer, K. S., Swartz, S. M. (2008). Quantifying the complexity of bat wing kinematics. *J. Theor. Biol.* 254, 604-615.
- Ros, I. G., Bassman, L. C., Badger, M. A., Pierson, A. N., and Biewener, A. A. (2011). Pigeons steer like helicopters and generate down-and upstroke lift during low speed turns. *Proc. Natl. Acad. Sci. U.S.A.*, 108, 19990-19995.
- Swaddle, J. P. (1997). Within-individual changes in developmental stability affect flight performance. *Behav. Ecol.* 8, 601-604.
- Tobalske, B. W. (2007). Biomechanics of bird flight. *J. Exp. Biol.* 210, 3135-3146.
- Tobalske, B., and Dial, K. (1996). Flight kinematics of black-billed magpies and pigeons over a wide range of speeds. *J. Exp. Biol.* 199, 263-280.
- Therialt, D. H., Fuller, N. W., Jackson, B. E., Bluhm, E., Evangelista, D., Wu, Z., Betke, M., Hedrick, T. L. (accepted). A method for accurate multi-camera field videography. *J. Exp. Biol.*
- Ward, S., Möller, U., Rayner, J. M. V., Jackson, D. M., Bilo, D., Nachtigall, W., and Speakman, J. R. (2001). Metabolic power, mechanical power and efficiency during wind tunnel flight by the European starling *Sturnus vulgaris*. *J. Exp. Biol.* 204, 3311-3322.
- Warrick, D. R. (1998). The turning-and linear-maneuvering performance of birds: the cost of efficiency for coursing insectivores. *Can. J. Zool.* 76, 1063-1079.
- Warrick, D. R., Dial, K. P., and Biewener, A. A. (1998). Asymmetrical force production in the maneuvering flight of pigeons. *Auk* 115, 916-928.
- Zeger, S. L., Liang, K. Y., and Albert, P. S. (1988). Models for longitudinal data: a generalized estimating equation approach. *Biometrics* 44, 1049-1060.